Published OnlineFirst October 3, 2014; DOI: 10.1158/1535-7163.MCT-13-1091

Molecular Cancer Therapeutics

Inhibition of Monocarboxylate Transporter-1 (MCT1) by AZD3965 Enhances Radiosensitivity by Reducing Lactate Transport

Becky M. Bola[1,2], Amy L. Chadwick[1,3], Filippos Michopoulos[4], Kathryn G. Blount[1], Brian A. Telfer[1], Kaye J. Williams[1], Paul D. Smith[4], Susan E. Critchlow[4], and Ian J. Stratford[1]

Abstract

Inhibition of the monocarboxylate transporter MCT1 by AZD3965 results in an increase in glycolysis in human tumor cell lines and xenografts. This is indicated by changes in the levels of specific glycolytic metabolites and in changes in glycolytic enzyme kinetics. These drug-induced metabolic changes translate into an inhibition of tumor growth *in vivo*. Thus, we combined AZD3965 with fractionated radiation to treat small cell lung cancer (SCLC) xenografts and showed that the combination provided a significantly greater therapeutic effect than the use of either modality alone. These results strongly support the notion of combining MCT1 inhibition with radiotherapy in the treatment of SCLC and other solid tumors. *Mol Cancer Ther; 13(12); 2805–16. ©2014 AACR.*

Introduction

The presence of hypoxia is a microenvironmental characteristic of the majority of solid tumors. A hypoxic microenvironment is associated with malignant progression, development of metastases, and presents a challenge for conventional cancer therapeutics (1–4). In addition to genetic changes acquired during tumor development, microenvironmental constraints can dictate the adaptive metabolic pathways used within a tumor. In particular, tumor hypoxia can direct the metabolic phenotype toward glycolysis. This glycolytic adaptation can persist even in the presence of oxygen in which it is referred to as the Warburg effect (5). This altered metabolic phenotype has recently been identified as an emerging hallmark of cancer (6). Increased glycolysis results in the generation of lactate, this is not only a waste product of increased glycolytic rate, but it is also thought to act as a signaling molecule, an antioxidant, and is reported to enhance immune escape (7). Consequently, increased tumor hypoxia, glycolytic rate, and lactate concentration are linked with tumor aggressiveness, treatment failure, and metastasis. In fact, lactate itself is a powerful independent prognostic indicator of disease progression, metastasis, and reduced survival in many tumor types (8–12).

Lactate production results in a requirement for lactate transport, both to prevent lactate accumulation and to provide a respiratory substrate. The majority of lactate transport occurs via the family of proton-linked monocarboxylate transporters (MCT) that are responsible for the facilitated diffusion of a carboxylate ion and a proton across the plasma membrane. This transport is not an active process and is reliant on the overall concentration gradient of the metabolite (13, 14). Of this family, MCT1 and MCT4 are the predominantly expressed isoforms in cancer. MCT1 has a ubiquitous expression pattern and mediates the bidirectional high-affinity transport of monocarboxylates, including L-lactate, pyruvate, acetate, and D,L-β-hydroxybutyrate (15). In contrast, MCT4 is hypoxia regulated; it has a lower affinity for lactate, a higher turnover rate, and is adapted toward lactate efflux in glycolytic cells (16, 17).

Lactate lost from one cell population can be taken up and used as a respiratory substrate in others. This metabolic cooperation is seen in some normal tissues such as in fast twitch muscle fibers [(refs. 18–20) and between neurons and glia (refs. 21–23)]. Analogous to this, increasing evidence suggests that lactate shuttling may play an important role in tumor growth and metastasis. Sonveaux and colleagues (24) hypothesized that a metabolic symbiosis may exist in solid tumors whereby lactate produced during glycolysis in the hypoxic tumor cell compartment is preferentially taken up by the oxygenated tumor cell population and used as a fuel source for oxidative metabolism. Similarly, it has been suggested that metabolic coupling may occur between aerobic tumor cells and the

[1]Manchester Pharmacy School, Manchester Cancer Research Centre, University of Manchester, Manchester, United Kingdom. [2]Clinical and Experimental Pharmacology, CR-UK Manchester Institute, Manchester, United Kingdom. [3]Breakthrough Breast Cancer, Institute of Cancer Sciences, University of Manchester, Manchester, United Kingdom. [4]Oncology iMED, AstraZeneca, Mereside, Cheshire, United Kingdom.

Note: Supplementary data for this article are available at Molecular Cancer Therapeutics Online (http://mct.aacrjournals.org/).

Corresponding Author: Ian J. Stratford, Manchester Pharmacy School, University of Manchester, Room 2.018, Stopford Building, Oxford Road, Manchester M13 9PT, UK. Phone: 44-0-161-275-2387; Fax: 44-0-161-275-2416; E-mail: ian.stratford@manchester.ac.uk

doi: 10.1158/1535-7163.MCT-13-1091

Published OnlineFirst October 3, 2014; DOI: 10.1158/1535-7163.MCT-13-1091

cancer-associated stroma within multiple cancer types, including cancers of the breast (5), ovary (25), and prostate (26). In this model, tumor cells are able to induce oxidative stress, glycolysis, upregulation of MCT4, and lactate efflux in cancer-associated fibroblasts, providing metabolic substrates for aerobic MCT1-expressing epithelial tumor cells. The transport of lactate is, therefore, critical to the maintenance of the symbiotic microenvironment and MCT1 is identified as the major transporter involved in lactate influx into tumor cells. In addition to the important functional role of MCT1 in tumor metabolism, MCT1 protein expression in tumors has been linked with variables associated with disease progression and prognosis in a variety of tumor types, including breast (27), ovarian (28), gastric (29), and colorectal cancers (30).

For these reasons, MCT1 is an attractive therapeutic target for inhibiting the metabolic interplay between cell populations within tumors. The nonspecific MCT1 inhibitor α-cyano-4-hydroxycinnamate (CHC) has been reported to produce antitumor effects by interfering with this metabolic coupling, by inhibiting lactate uptake into oxygenated tumor cells, increasing glucose uptake, and indirectly starving hypoxic tumor cells of glucose (24). In addition, CHC has been shown to increase necrosis and alter tumor volume *in vivo* (31–33). However, CHC is not a specific MCT1 inhibitor and as a consequence these data should be interpreted with caution (34, 35).

Specific inhibitors with greater inhibitory potency and selectivity toward MCT1 have been developed for use in immunosuppression (36, 37), and these have been shown to influence lactate transport (38). Recent improvements on these compounds have resulted in the generation, by AstraZeneca, of AZD3965. This compound is a selective MCT1 inhibitor; it inhibits MCT1 with a binding affinity of 1.6 nmol/L and it is 6-fold more selective over MCT2 and does not inhibit MCT3 or 4 at 10 mmol/L concentrations (39). In addition, the compound has good oral bioavailability, and it has entered the phase I clinical trial for treatment of advanced solid tumors (40).

In this study, we evaluate the metabolic and therapeutic effects of AZD3965 in small cell lung cancer (SCLC) and gastric cancer cell lines. In particular, we demonstrate the ability of AZD3965 to inhibit both lactate efflux and influx into cells and cause an increase in glycolysis and an upregulation of glycolytic enzymes. These changes were sufficient to inhibit tumor growth *in vivo*. In addition, we combined AZD3965 with radiotherapy *in vivo* and showed that the combined treatment produced a substantially greater antitumor effect than either modality when used alone.

Materials and Methods

Cells

DMS114 and H526 SCLC cells and HGC27 gastric cancer cells were maintained in RPMI-1640 with 10% FCS and 1% L-glutamine (complete media). Cell lines were chosen on the basis of relatively high sensitivity to AZD3965 (39). DMS114 and HGC27 cells were obtained from AstraZeneca and H526 cells were provided by the CR-UK Manchester Institute (Manchester, UK). All cells were subsequently authenticated while used in the University of Manchester laboratories by the use of an in-house DNA sequencing and authentication service. Cells were also shown to be mycoplasma free during the course of this work. For all experiments, cells were plated overnight before treatment with AZD3965 and/or different oxygen concentrations for a further 24 hours (unless an alternative treatment time is indicated). Some experiments also included exposure to cobalt chloride as a hypoxia-mimetic. Cobalt chloride is able to mimic hypoxia by preventing HIF degradation, this is at least partially due to its occupation of the VHL-binding domain of HIF1α, thus preventing its degradation (41).

Glucose and lactate uptake assay

After treatment cells were washed before the addition of uptake cocktail consisting of buffer (25 mmol/L glucose, 137 mmol/L NaCl, 5.37 mmol/L KCl, 0.3 mmol/L Na_2HPO4, 0.44 mmol/L KH_2PO_4, 4.17 mmol/L $NaHCO_3$, 1.26 mmol/L $CaCl_2$, 0.8 mmol/L $MgSO_4$, and 10 mmol/L HEPES pH 7.4) containing 100 nmol/L AZD3965 or equivalent volume of DMSO vehicle. For the glucose and lactate assays, 2 mmol/L glucose and ^{3}H-2-deoxyglucose at an activity of 2μCi and ^{14}C-lactate at an activity of 0.2μCi were added, respectively, and incubated for 1 hour at 37°C. Subsequently, the cocktail was removed and the cells washed and lysed in 0.5 mL of lysis buffer (0.1% SDS and 0.1% Triton-X in HEPES buffer); 0.4 mL of this was transferred to a scintillation vial with 4 mL of scintillation fluid (Ecoscint A; National Diagnostics), the addition of 0.4 mL of the original lactate or glucose cocktail was used as a positive control, to establish the total amount of radioactive metabolite added. The remaining 100 μL was used for a protein assay. The uptake was normalized to both the amount of radioactive metabolite present in the media (positive control) and also to protein concentration, to control for variation in cell number, which may have been caused as a result of the treatments.

Lactate, ATP, and GSH/GSSG assay

Lactate concentration was determined by colorimetric assay (Trinity Biotech) and compared with a standard curve of known lactate concentrations. The lactate present as a result of efflux from the cell was determined by measuring cell-free samples and deducting the amount of lactate originally in the media (derived from the FCS). Intracellular lactate was evaluated using the same assay; cells were washed in PBS before lysis in Tris/NaCl lysis buffer (20 mmol/L Tris, 150 mmol/L NaCl, 1% Triton-X100, pH 7.6).

The ATP concentration in cell lysates was determined by a luminescent assay (ENLITEN ATP system;

Published OnlineFirst October 3, 2014; DOI: 10.1158/1535-7163.MCT-13-1091

Promega) and comparison made with the cellular ATP concentrations in lysates derived from untreated normoxic controls.

GSH and GSSG (glutathione and oxidized glutathione) concentrations were determined according to manufacturer's instructions by GSH/GSSG-Glo luminescent assay (Promega).

Assay of reactive oxygen species

Following treatment cells were resuspended in PBS and stained with 10 μmol/L carboxy-DCFDA (Molecular Probes; Invitrogen), washed and then 10,000 events within a population gated to only include live cells was analyzed by FACs (Cyan ADP flow cytometer). Mean fluorescence in the live cell population was compared against the control for each oxygen tension and drug concentration.

Metabolomics

Cells were plated and allowed to adhere before washing and exchanging the media for one containing dialyzed FCS devoid of constituents smaller than 1,000 amu such as small sugars and lactate (Sigma-Aldrich). Hypoxic (1% oxygen) experiments were conducted in a hypoxic cabinet (Ruskinn Sci-tive-N). Samples were treated with DMSO vehicle, 10 nmol/L or 1 μmol/L AZD3965 for 6 or 24 hours under normoxic or hypoxic conditions. To extract the metabolites media were removed and 400 μL (−20°C) 40:40:20 acetonitrile:-methanol:water added immediately to quench metabolism and extract metabolites. The plates were then kept on dry ice for 20 minutes before scraping the cell:solvent mixture into chilled tubes, precipitated proteins were then removed by centrifugation and the supernatant stored at −20°C. As an LC/MS quality control (QC), a pooled sample was generated containing equal quantities of each sample. Samples (100 μL) and the pooled sample were evaporated using a SpeedVac Savant 1010 (Thermo Scientific), with no heat, for 60 minutes. Subsequently, metabolites were resuspended in 50 μL deionized water. For the liquid chromatography a Dionex U3000 RS pump was operated at 400 μL/min and the column maintained at 60°C. Liquid chromatography used: Buffer A, 10 mmol/L tributylamine, 15 mmol/L acetic acid in water; and buffer B, 20% isopropanol in methanol; column: waters acquity HSS C18 100 × 2.1 mm, 1.7-μm particles. Metabolites were eluted following a gradient profile starting at 0 to 0.5 minutes at 0% B changing after 4 minutes to 5% B, 6 minutes 5% B, 6.5 minutes 20% B, 8.5 minutes 20% B, 14 minutes 55% B, 15 minutes to 100% B, and column flushed with 100% B for another 2 minutes before changing to 100% A for 3 minutes reequilibration before next injection. After the column was conditioned using 10 injections of the pooled sample, all samples were analyzed in random order on a 4000 Qtrap mass spectrometer using negative ionization. A QC sample was injected every 10 samples to monitor instrument variability. Subsequently, peak integration was performed using the MultiQuant software and all sample peaks were compared with the standards (and standards + QC mix to ensure that the correct peak was selected). Data were further scaled to log-base 2 and normalized to the median sample metabolic profile. Coefficients of variation (CV; SD/mean × 100) were calculated for each QC analyte. Fold changes, F test, and T tests between groups were calculated using Excel. Metabolites are considered to have changed when they met the following criteria: (i) QC CV < 30; (ii) a P value of <0.05 and absolute $\log_2$ (fold change) > 0.5 (log fold change calculated using the following formula: [average(treated)]-[average(group; DMSO control)].

Determination of glycolytic enzyme kinetics

Cells were plated overnight and treated with 100 nmol/L AZD3965 or vehicle for 24 hours. The cells were then washed, once in PBS and twice with lysis buffer [50 mmol/L Mops, 100 mmol/L KCl, 5 mmol/L $MgCl_2$, 1 mmol/L EDTA, 0.1 mmol/L DTT, and 1 mmol/L PMSF supplemented with 1x mini complete protease inhibitor cocktail tablets (Roche)]. The cells were harvested by scraping and centrifugation, and the pellet snap frozen without buffer in liquid nitrogen. Frozen aliquots of cells were thawed on ice and resuspended in lysis buffer. Cells were lysed by three rounds of freezing in liquid nitrogen and thawing at 37°C for 2 minutes each. Lysates were subsequently centrifuged (13,000 g, 10 min, 4°C) until clear and then stored on ice. Enzyme activity in the cell lysates was determined using a micro-plate reader (Anthos Zenyth 3100) to measure either production or depletion of NADH/NADPH, through its absorbance at 340/10 nm, occurring as a result of direct or coupled enzyme reactions. The 96-well plates used for the assays were preheated to 37°C for 10 minutes before starting reactions, initiated by the addition of 5 μL cell lysate to 95 μL of reaction buffer (50 mmol/L Mops pH 7.4, 100 mmol/L KCl, and 5 mmol/L free magnesium). The standard reaction buffer was supplemented (for details see Supplementary Table S1) to assay the kinetics of the different enzymes. Data were processed using MatLab v.2011a. Absorbance values for controls were subtracted from absorbance of corresponding reactions. Gradients (Δabsorbance/Δtime) of the linear portion of the initial rates were calculated and divided by the extinction coefficient of NADH/NADPH [6.220 (per mmol/L)/cm] to give the initial rate V_o values. Absorbance readings were normalized to give a path length of 1 cm. Initial (V_o) rates were calculated using KINETICSWIZARD (40). GraphPad prism 6 was used to plot V_o values against substrate concentration and determine V_{max} and K_m values. The V_{max} was then normalized to the protein concentration in the cell lysate.

Tumor responses *in vivo*

Adult (8 weeks +) female CD-1 nude mice (Charles River Laboratories) were implanted with 0.1 mL of H526 cells at 5×10^7 cells mL/L. Cells were implanted

Published OnlineFirst October 3, 2014; DOI: 10.1158/1535-7163.MCT-13-1091

s.c. in the mid-dorsal region and when tumor volumes reached 150 mm^3 the mice were assigned treatment groups (up to 8 mice/group) and tumor measurements subsequently made daily. About 100 mg/kg AZD3965 was administered twice daily by oral gavage for a total of 7 days. This drug dose was chosen on the basis of being well tolerated and maintaining MCT1 inhibition over a 7-day period (39). On the third day of drug or vehicle treatment, mice received 2 Gy locally to the tumor for 3 successive days (3 × 2 Gy). In the radiation-alone group the radiation was administered on the third day after the tumor volume reached 150 mm^3. Radiation treatment was given using a metal–ceramic MXR-320/36 X-ray machine (320 kV; Comet AG) as previously described (42). At the end of the 7-day treatment period, 3 mice from each group were sacrificed for histologic analysis of tumors. The remaining mice in each group were kept on study until tumors reached a volume of 1,000 mm^3.

Animal study protocols were approved by the Institutional Ethics Committee and the Home Office (project license 40/3212,) and designed in accordance with the Scientific Procedures Act (1986) and the 2010 guidelines for the welfare and use of animals in cancer research (43).

IHC analysis

Tumors were harvested and snap frozen in two pieces in liquid nitrogen within 2 minutes of sacrifice. The tumors were cut into 10-μm sections using a OFT5000 cryostat (Bright), fixed in chilled acetone, and stained for MCT1, MCT4 [in-house (AstraZeneca) polyclonal antibodies], and CD31 (rat anti-mouse CD31; Pharmingen, BD Biosciences).

Statistical analysis

Kaplan–Meier plots were evaluated using the log-rank (Mantel–Cox) test; otherwise significance was determined using an unpaired two-tailed Student *t* test for two-sample equal variance.

Results

AZD3965 inhibits bidirectional lactate transport

AZD3965 (Supplementary Fig. S1) was designed to selectively inhibit MCT1 and would, therefore, be expected to influence the movement of lactate into and out of cells. In the first instance, the effect of AZD3965 on lactate efflux was studied. Equivalent numbers of cells were incubated in either normoxia, 1% oxygen (hypoxia), or anoxia in complete media supplemented with AZD3965 or DMSO vehicle for 24 hours. After this time media and cells were collected to determine lactate concentrations. Generally, treatment with AZD3965 caused an increase in intracellular lactate (Fig. 1A–C). There was a corresponding trend for reduction of extracellular lactate concentration, but these changes were not significantly different; this may have been due to the inherent difficulty in measuring extracellular lactate in media that already contain significant amounts of serum-derived lactate (Fig. 1D–F).

As MCT1 is a bidirectional transporter (13), the effects of AZD3965 on lactate influx were determined using a radioactive assay that measured the amount of lactate taken up by the cell (when other respiratory substrates were available) over 1 hour. Figure 2A and B shows the effect of 24 hours treatment with AZD3965 on subsequent uptake of lactate. A significant decrease in lactate uptake was observed when the drug was administered 24 or 4 hours before, or the same time as, the radioactive lactate (defined as acute in Fig. 2E and F). These experiments suggest that AZD3965 inhibits lactate transport by MCT1 regardless of the direction of lactate movement. Figure 2 also shows that inhibition of lactate uptake was seen when the hypoxia mimetic cobalt chloride was applied to the cells concurrently with AZD3965, this suggests that the HIF1-mediated induction of MCT4 does not counteract the effect of the drug on lactate influx. This also suggests that even in the hypoxic regions of tumors, in which MCT4 might be upregulated, there might be significant inhibition of lactate uptake.

It is possible that the reduction in lactate uptake could contribute to the reduction in lactate efflux. This is because the reduction in lactate uptake creates a requirement for increased glycolysis to supply TCA cycle substrates, which must be immediately used by, and not lost from, the cell.

Metabolic analysis of the effect of inhibiting lactate transport

To determine the effects of inhibiting lactate transport on other metabolic pathways, 116 intracellular metabolites were analyzed using LC/MS (for details see Supplementary Information). Samples were prepared 6 and 24 hours after the addition of 10 nmol/L or 1 μmol/L AZD3965 or DMSO control in both normoxia and hypoxia. A hierarchical analysis of the levels of individual metabolites under each experimental condition is provided in Supplementary Fig. S2. The data were processed using an in-house model (the AstraZeneca pathway annotation tool). This model considered 41 metabolic pathways, and the change in metabolite levels in each pathway was calculated. In this analysis, the extent to which a pathway is altered is determined by measuring the number of metabolites that demonstrate a significant change (see below) between the two samples that are being compared (indicated on the left hand side of the heat map in Fig. 3). The greater the alteration, the brighter the color assigned on the heatmap. Larger changes in metabolism were observed when the treatment with AZD3965 was conducted under hypoxic conditions consistent with the increased requirement for lactate transport under these conditions. Also, greater changes were observed when the drug treatment was relatively short (6 hours) as opposed to longer exposure times (24 hours).

Published OnlineFirst October 3, 2014; DOI: 10.1158/1535-7163.MCT-13-1091

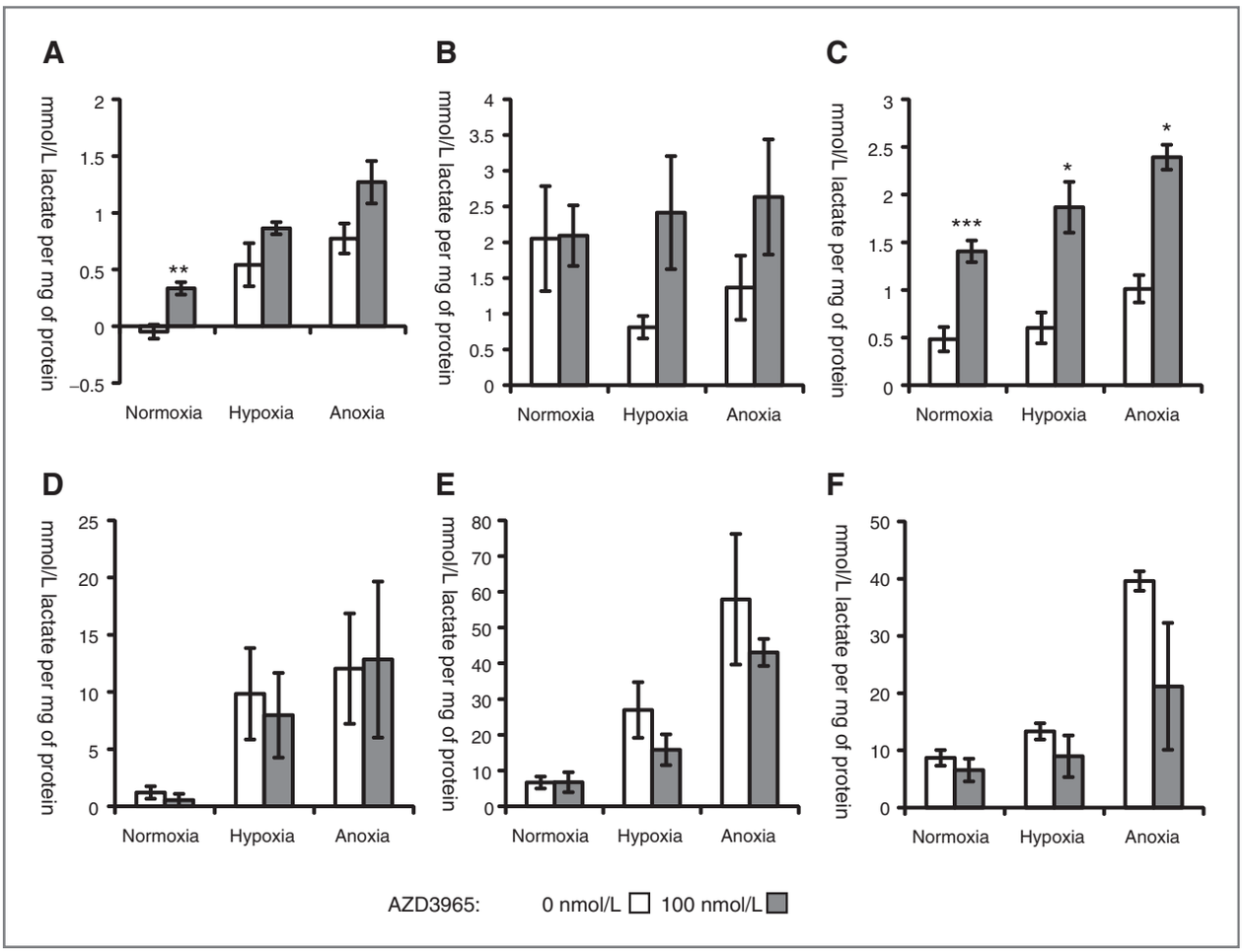

Figure 1. AZD3965 increases intracellular lactate while decreasing the amount of extracellular lactate. Cells were treated with 100 nmol/L AZD3965 in normoxia, hypoxia, or anoxia for 24 hours before determining lactate concentrations. Intracellular lactate (A–C); extracellular lactate (D–F). H526 cells (A and D); HGC27 cells (B and E); and DMS114 cells (C and F). *, $P < 0.05$; **, $P < 0.01$; ***, $P < 0.001$, significantly different; drug-treated versus controls. Mean and SEMs are derived from three independent experiments.

In the hypoxic samples, significant changes were observed in pathways involved in amino acid metabolism, such as: alanine, aspartate, glutamine, arginine, proline, and β-alanine, as well as amino-acyl tRNA biosynthesis and amino acid and nucleotide sugar metabolism. These data are consistent with previous reports of a shift to an anabolic phenotype caused by oxidative stress mediated by effects on the pentose phosphate pathway (PPP; refs. 44, 45). Consistent with this, changes in PPP were also observed.

To consider whether the increased effects seen in the hypoxic samples are simply a reflection of the metabolic changes brought about by the hypoxic environment, the hypoxic samples were compared with their normoxic counterparts (matched for time and drug concentration). This analysis (shown in Supplementary Fig. S3) also demonstrated evidence of a shift to an anabolic phenotype. This suggests that the comparable shift brought about by the drug could be as a result a heightened sensitivity of the cells to hypoxia as a result of treatment with AZD3965. Hypoxia also resulted in some changes to glycolytic intermediates; however, changes in glycolysis as a result of treatment with AZD3965 were observed in every 6-hour time point. Inspection of the individual metabolite levels indicated that there was a dose-dependent increase in the concentration of intermediates early in the glycolytic pathway, and a similar dose-dependent decrease in those appearing late (for example, pyruvate seen in Fig. 4). The metabolite changes observed as a result of the treatment with AZD3965 are in the same direction as, but lesser in magnitude compared with the changes caused by hypoxia. As hypoxia is generally associated with an increase in glycolytic rate, this would suggest that the changes seen are indicative of a more glycolytic phenotype (46). The drug dose–dependent nature of these changes, coupled with fact that there are dose-dependent increases in both of the early glycolytic intermediates measured (glucose-6-phosphate

Published OnlineFirst October 3, 2014; DOI: 10.1158/1535-7163.MCT-13-1091

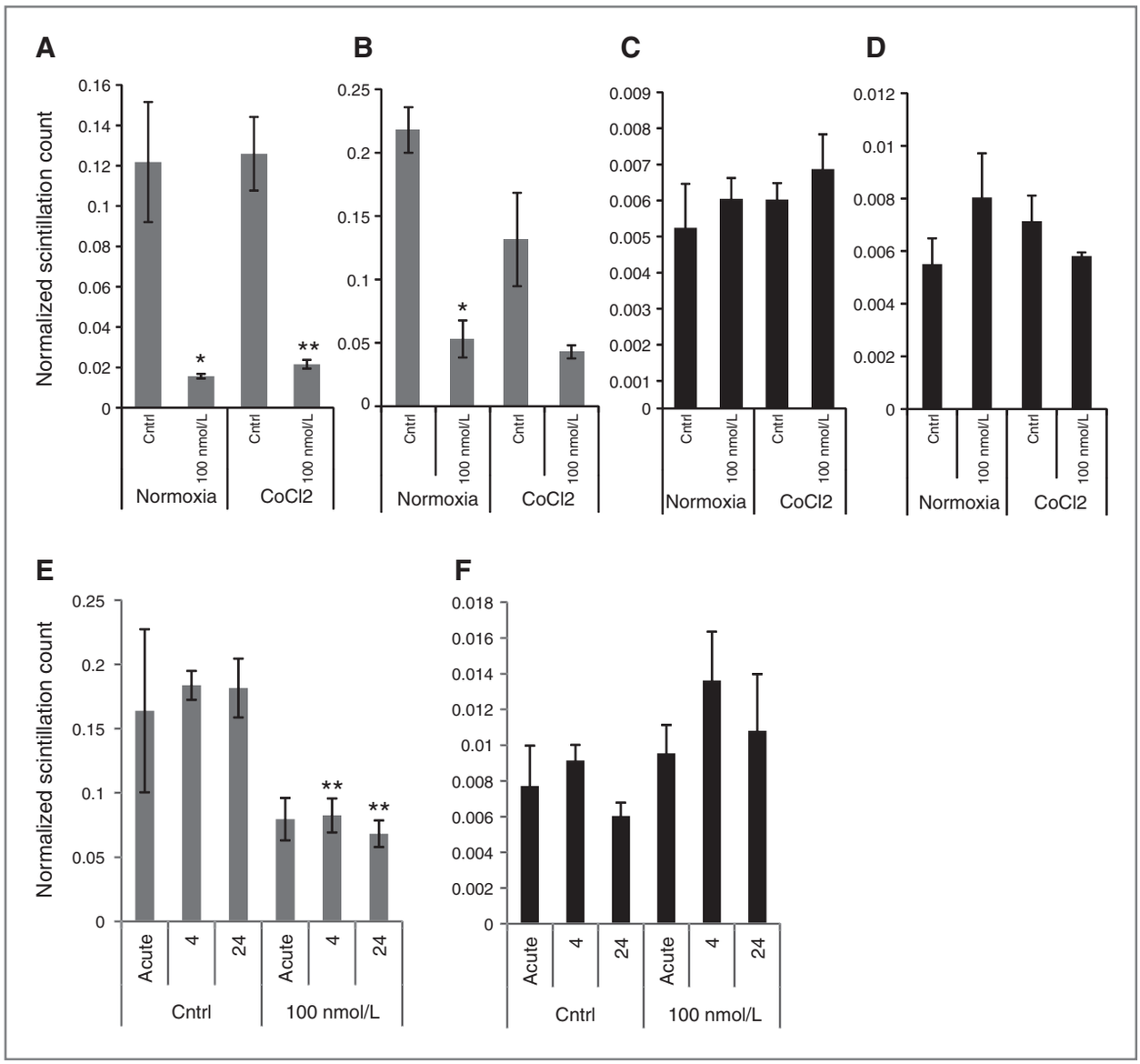

Figure 2. AZD3965 significantly reduces lactate uptake. The uptake of lactate (A and B) and glucose (C and D) was measured 24 hours after exposure to AZD3965 in the presence or absence of cobalt chloride. A and C, DMS114 cells; B and D, HGC27 cells. E and F, time course assays, in which AZD3965 was applied for the number of hours indicated; "acute" dosing is when drug was administered concomitant with radiolabeled metabolite. Lactate (E), and glucose (F). *, $P < 0.05$; **, $P < 0.01$, significantly different; drug-treated versus controls. Mean and SEMs derived from three independent experiments.

and fructose-1-phosphate, see Fig. 4), provide confidence in this conclusion.

We then analyzed the effect of inhibting lactate transport on glycolytic enzyme kinetics (Fig. 4). Changes in V_{max} of both pyruvate kinase and hexokinase were demonstrated; however, for hexokinase there was no accompanying change in K_m, and the K_m change with pyruvate kinase was lower than the change in V_{max}. Increases in V_{max} indicate changes not in the kinetics of the enzyme reaction, but in the amount of enzyme present. These changes are partiularly noticable in the case of hexokinase, the first enzyme in the glycolytic cascade. An upregulation of hexokinase protein expression would be consitent with the increases in concentration of glucose-6-phosphate and fructose-1-phosphate. These expression changes would suggest that there has been a fundamental metabolic shift resulting in increased glycolysis in response to inhibition of lactate transport by AZD3965.

AZD3965 treatment results in increased oxidative stress

The metabolic changes observed above suggested that treatment of cells with AZD3965 could result in

Published OnlineFirst October 3, 2014; DOI: 10.1158/1535-7163.MCT-13-1091

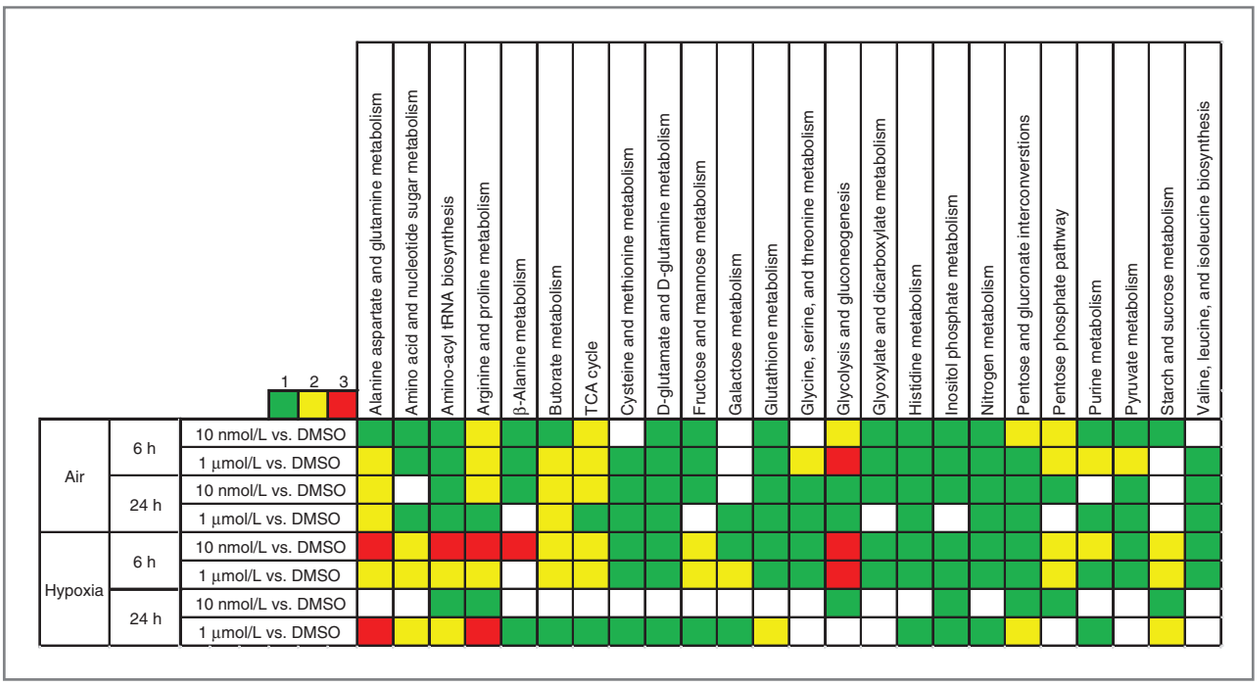

Figure 3. The effect of inhibiting lactate transport on metabolism. The heatmap, the extent of change in a pathway when the two conditions indicated in the right hand column are compared. The colors, the number of the metabolites in that pathway that shows a significant change in concentration. No weighting is given to the extent or the direction of the change in the levels of individual metabolites.

changes in cellular redox and cause oxidative stress. To evaluate this, we measured cellular levels of ATP, GSH/GSSG, and the generation of reactive oxygen species (ROS) following treatment of cells with AZD3965 in air, hypoxia, and anoxia (results are given in Supplementary Fig. S4). Anoxia alone results in a 50% reduction in cellular ATP and AZD3965 appears to cause a further decrease in ATP; in normoxia, 1 μmol/L AZD3965 causes a statistically significant 30% reduction in ATP. We further evaluated levels of GSH and GSSG; in air, AZD3965 has little effect on glutathione levels whereas in hypoxia a drug-dependent increase in the level of GSSG is observed. These changes in cellular redox were broadly reflected by the generation of ROS. In air, there was a decrease in ROS production following treatment with 1 μmol/L AZD3965, whereas in anoxia drug treatment led to a 50% increase in ROS. The different effects in air and anoxia probably indicate the different requirement of lactate transport under the different conditions. Interestingly, these changes in redox and ROS production are not sufficient to mediate cytotoxicity (Supplementary Methods and Supplementary Fig. S5).

Treatment of tumors *in vivo* with AZD3965 causes increased lactate concentration, a reduction in growth and increased radiation sensitivity.

Using conventional *in vitro* culture conditions, in which glucose is abundant, cells are better able to compensate for the inhibition of lactate uptake. In contrast in tumors, cells are exposed to nutrient (oxygen) limitations as cells move further way from a functional vascular supply. Under these conditions it is likely that the use of lactate as a respiratory substrate is critical for tumor cell survival. This concept of metabolic symbiosis has been described by Sonveaux and colleagues (24), who suggested that hypoxic cells undergoing glycolysis will provide the aerobic fraction of a tumor with lactate to use as a respiratory substrate. This symbiosis has two advantages, first this allows the hypoxic, glycolytic fraction to benefit from sufficient glucose, but it also prevents acidification of the extracellular space that could be caused by lactate accumulation. In this model, MCT1 is likely to be pivotal to this shuttling of lactate between tumor compartments; hence, the efficacy of AZD3965 was investigated *in vivo*.

Mice bearing H526 tumors were treated with AZD3965 for 7 days. Figure 5A shows that treatment with AZD3965 resulted in a delay in tumor growth. Analysis of the time taken for individual tumors to grow from 150 to 1,000 mm^3 showed that this was 8 days for tumors in mice treated with vehicle alone compared with 12 days for those given AZD3965 ($P = 0.004$, Fig. 5B). One mouse in the treatment group was cured and omitted from this analysis. However, a Kaplan–Meier plot of AZD3965 treatment efficacy, in which survival was linked to tumor size (with animals sacrificed when tumors reached 1,000 mm^3), also showed significance ($P = 0.008$). Tumors were harvested at the end of drug treatment, and at this time, higher concentrations of tumor lactate were found in the group that had received

Published OnlineFirst October 3, 2014; DOI: 10.1158/1535-7163.MCT-13-1091

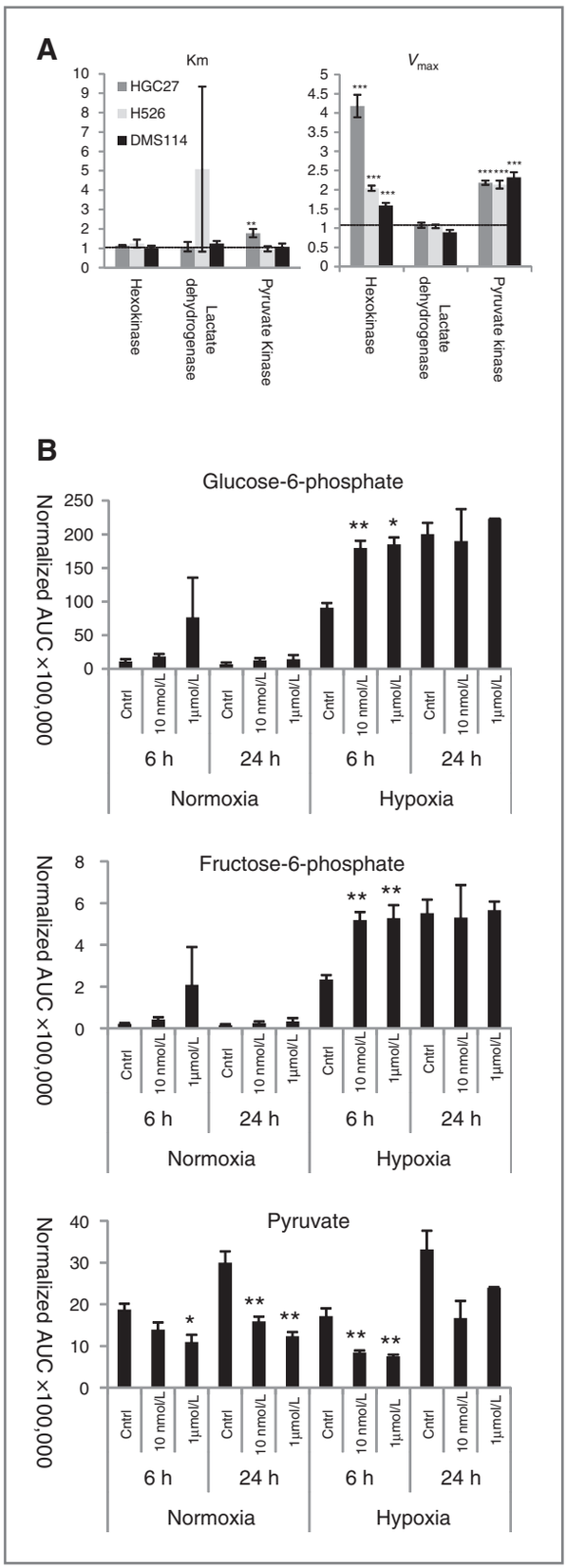

the AZD3965, suggesting *in vivo* efficacy in inhibiting lactate transport (Fig. 6A). To ensure that this difference was not due to changes in angiogenesis, IHC analysis of CD31 was used to assess vessel number, size, and overall coverage. Figure 6B shows that there were no significant drug-induced changes in vessel number and similarly there were no changes in vessel size or coverage (Supplementary Fig. S6). Thus, it is likely that the changes in lactate observed were a specific effect of MCT inhibition and not due to any changes in angiogenesis. Interestingly, a significant ($P < 0.05$) increase was observed in the extent of MCT4 staining (Fig. 6C) and this occurred without an increased hypoxia, as measured by pimonidazole binding (data not shown), suggesting that the upregulation of MCT4 is not due to increased tumor hypoxia but rather indicative of increased glycolysis. This is consistent with our *in vitro* observations and the use of MCT4 as a glycolytic marker, which has been published previously (47).

We have shown above that treatment of anoxic cells with AZD3965 can profoundly alter their redox status. This, together the fact that AZD3965 will perturb the metabolic symbiosis between the hypoxic and aerobic cells within the tumor, strongly suggests that the hypoxic/anoxic cells may be more vulnerable to adjuvant treatment. Because the effectiveness of radiotherapy is limited by the resistance of the hypoxic/anoxic cells (1), a combination of AZD3965 with radiotherapy could be beneficial. To test this, H526 xenografts were grown to a volume of 150 mm^3; one group of mice received no treatment for 2 days followed by three daily fractions of 2 Gy (3×2 Gy); the second group received AZD3965 for 2 days followed by AZD3965 together with 3×2 Gy fractionated radiotherapy followed by 2 further days of AZD3965. Mice were sacrificed at the end of drug treatment or tumors were allowed to grow to 1,000 mm^3. In all cases, tumors were harvested for IHC analysis or assessment of lactate levels. At the end of the treatment period there was a considerable increase in the lactate levels observed in the tumors treated with AZD3965 (Fig. 7A). In comparison with Fig. 6, radiation alone has no discernible effect on tumor lactate levels.

Administration of AZD3965 alone for 7 days increased the time for tumors to reach 1,000 mm^3 from 8 to 12 days (Fig. 5); for radiation alone this time was 18 days, which was increased to 25 days when combined with AZD3965 ($P = 0.02$, Fig. 7B). Growth curves

Figure 4. Inhibiting lactate transport increases glycolytic rate. A, glycolytic flux analysis was used to compare the activity of three key glycolytic enzymes. K_m and V_{max} were calculated and are expressed as a ratio of the control cells to the cells treated for 24 hours with 100 nmol/L AZD3965; horizontal line, a value indicative of no change as a result of treatment with AZD3965. B, the concentrations of the individual metabolites measured in the glycolytic pathway [values represent area under curve (AUC) normalized to median AUC]. Mean and SEMs derived from three independent experiments. *, $P < 0.05$; **, $P < 0.01$; ***, $P < 0.001$, significantly different; drug-treated versus controls.

Published OnlineFirst October 3, 2014; DOI: 10.1158/1535-7163.MCT-13-1091

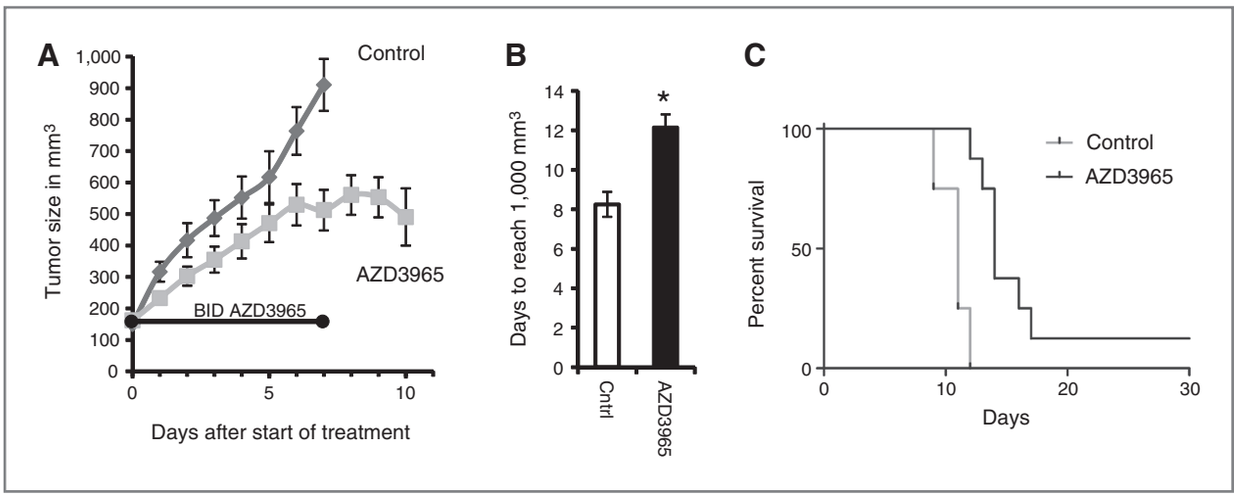

Figure 5. AZD3965 slows H526 xenograft growth *in vivo*. A, *in vivo* growth curves showing tumor volume (mean and SEM) in mm^3 after start of treatment; the growth curve finishes when the first tumor in each group reaches 1,000 mm^3. The control group contained 5 mice, the AZD3965 group contained 11 mice, 3 of which were sacrificed for histology at the end of drug treatment (day 7). B, days (±SEM) taken to reach 1,000 mm^3 for each treatment group (*, $P = 0.004$, significantly different). In the AZD3965 group, 1 mouse was cured and observed for a further 100 days after the tumor ceased to be visible and no tumor returned. This reduction in tumor size resulted in the apparent dip at the end of the AZD3965 growth curve and is why the Kaplan–Meier plot (C) does not reach zero for the AZD3965 group.

are given in (Fig. 7C). Kaplan–Meier analysis (Fig. 7D) showed that the difference in survival between the mice treated with radiation only compared with the group receiving radiation plus AZD3965 was significant ($P = 0.011$). Clearly, the therapeutic effect of combining AZD3965 with radiotherapy is greater than using either modality individually.

Discussion

Sonveaux and colleagues (24) used the nonspecific MCT1 inhibitor CHC to propose a model whereby inhibition of lactate influx resulted in a switch from lactate fuelled oxidative metabolism to glycolysis in the oxygenated regions of the tumor. They demonstrated that, in oxygenated regions, lactate was used as a fuel source in preference to glucose whereas, when MCT1 was inhibited, the cells adopted a glycolytic phenotype using glucose as their fuel source. These data were of considerable importance for highlighting the potential therapeutic importance of inhibiting lactate transport; however, despite the rigorous controls used by the authors there were still some concerns about the overall conclusions as CHC is not a specific inhibitor of MCT1. One of the off-target effects of CHC is inhibition of the mitochondrial pyruvate carrier. This inhibition is possible at the concentrations used in the study by Sonveaux and colleagues (24), and could explain the

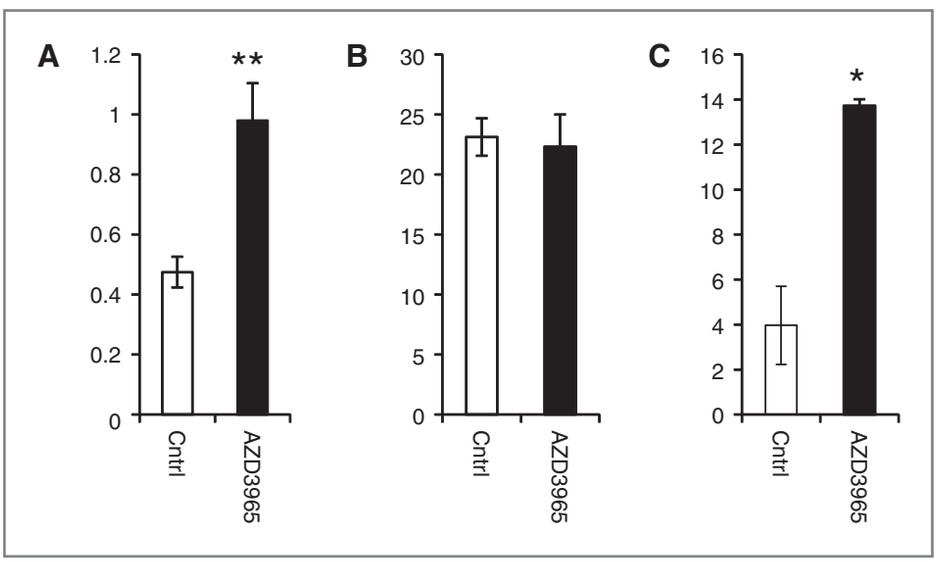

Figure 6. Effect of AZD3965 on lactate concentration, blood vessel density, and MCT4 expression in H526 xenografts. A, lactate concentration expressed as mmol/L lactate per mg of protein; B, mean number of blood vessels per image of the tumor as visualized using the endothelial cell marker CD31; C, proportion of tumor stained for MCT4. *, $P < 0.05$; **, $P < 0.01$, significantly different; drug-treated versus controls.

Published OnlineFirst October 3, 2014; DOI: 10.1158/1535-7163.MCT-13-1091

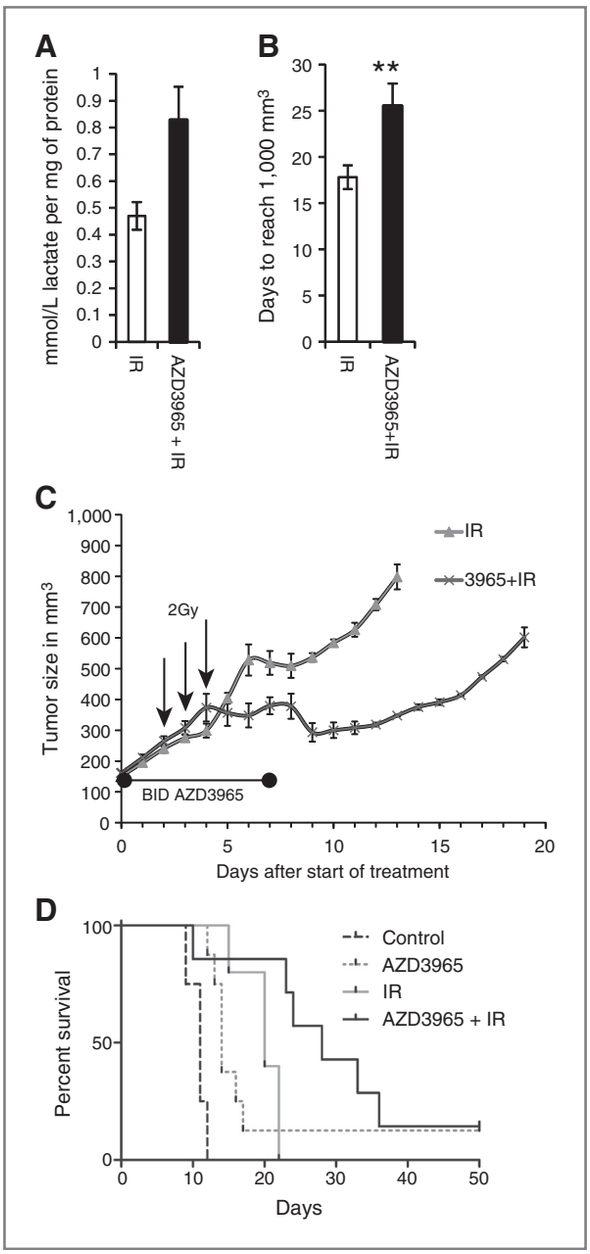

Figure 7. Combining AZD3965 with radiation to treat H526 xenografts. A, tumor lactate concentration at the end of drug treatment ($P = 0.14$); B, days taken to reach 1,000 mm^3 (mean and SEM, cured tumor not included); **, $P = 0.02$, significantly different; drug plus radiation versus radiation alone. The radiation-only group contained 8 mice, 3 of which were sacrificed at the end of the treatment period (7 days) for histology; the radiation plus AZD3965 group contained 10 mice, 3 of which were sacrificed at the end of drug treatment for histology. C, *in vivo* growth curves showing tumor volume in mm^3 (mean and SEM); the growth curve finishes when the first tumor reaches 1,000 mm^3. The 2-Gy fractions of radiation were delivered midway between the two doses of AZD3965 on the days indicated with an arrow. In the AZD3965 + radiation group, 1 mouse was cured and observed for a further 100 days after the tumor ceased to be visible and no tumor returned. This is why the Kaplan–Meier plot (D) does not reach zero for the AZD3965 group; the dotted lines are taken from Fig. 5, with both experiments being carried out at the same time.

inhibition of lactate oxidation observed (34). In contrast, AZD3965 is a specific MCT1 inhibitor and therefore, we are able to demonstrate, unambiguously, that the abrogation of the symbiotic tumor microenvironment can be achieved by the inhibition of lactate transport by MCT1.

We have demonstrated that AZD3965 is able to inhibit lactate transport both into and out of the cell with the greater effect observed on lactate uptake. These data are concordant with the majority of published observations regarding the role of MCT1 in lactate transport (13, 15, 24, 48), and thus treatment with AZD3965 will restrict lactate availability as a fuel source for aerobic metabolism. This metabolic change would force those cells using lactate to use an alternative fuel, for example, glucose, thus increasing the rate of glycolysis. This hypothesis is supported by the observation that treatment with AZD3965 resulted in changes in glycolytic metabolites determined by metabolomics analysis, an upregulation of glycolytic enzymes measured by glycolytic flux analysis, and an increase in the rate of glucose uptake (although this was not statistically significant). In keeping with this, the increase in cellular lactate that is observed could be due to an increase in glycolysis.

Inhibition of lactate transport resulted in a significant increase in tumor lactate *in vivo* and this effect was not as a result of perfusion changes brought about by changes to the blood vessels in the tumor. Moreover at the end of the treatment period a significant increase in MCT4 staining was observed; MCT4 is often considered a marker of glycolysis (47), and as such is concordant with previous observations surrounding increases in glycolytic rate. Despite the relatively brief treatment period (7 days), AZD3965 was also able to produce a statistically significant inhibition of tumor growth as a monotherapy.

On the basis of our hypotheses, AZD3965 would be particularly effective at killing the hypoxic areas of the tumor, as these would be the areas that would be starved of glucose when the aerobic fraction is unable to use lactate as a metabolic substrate. Moreover, the reduced cellular ATP, the increased percentage of GSSG, and the increase in ROS in anoxic conditions are indicative of cells experiencing oxidative stress and as such these cells would be more sensitive to radiotherapy. As a consequence, AZD3965 was combined with radiotherapy. When mice bearing tumors were treated with AZD3965 concurrently with 3 × 2 Gy radiotherapy and with AZD3965 alone for 2 days either side of the radiation treatment, a significant decrease in tumor growth was observed in the AZD3965 combined with the radiation group when compared with the groups that received either drug or radiation alone.

There is recent work describing the potential importance of metabolic symbiosis as important factor for sustaining tumor growth (49). It is likely that treatment of tumors with AZD3965 will perturb this symbiosis with the result of decreased tumor growth and

Published OnlineFirst October 3, 2014; DOI: 10.1158/1535-7163.MCT-13-1091

enhancement of the effects of radiotherapy. Inhibition of MCT1 with AZD3965 represents a novel method of specifically targeting solid tumors by pinpointing weaknesses inherent in the tumor microenvironment and this suggests that systemic administration in combination with targeted radiotherapy could represent an effective therapeutic strategy.

Disclosure of Potential Conflicts of Interest

P.D. Smith has ownership interest (including patents) in AstraZeneca. I.J. Stratford reports receiving commercial research grant from AstraZeneca. No potential conflicts of interest were disclosed by the other authors.

Authors' Contributions

Conception and design: B.M. Bola, A.L. Chadwick, P.D. Smith, S.E. Critchlow, I.J. Stratford
Development of methodology: B.M. Bola, A.L. Chadwick, F. Michopoulos, B.A. Telfer
Acquisition of data (provided animals, acquired and managed patients, provided facilities, etc.): B.M. Bola, A.L. Chadwick, F. Michopoulos, K.G. Blount, B.A. Telfer, K.J. Williams
Analysis and interpretation of data (e.g., statistical analysis, biostatistics, computational analysis): B.M. Bola, A.L. Chadwick, F. Michopoulos, K.G. Blount
Writing, review, and/or revision of the manuscript: B.M. Bola, A.L. Chadwick, K.J. Williams, P.D. Smith, S.E. Critchlow, I.J. Stratford
Administrative, technical, or material support (i.e., reporting or organizing data, constructing databases): B.M. Bola
Study supervision: B.M. Bola, B.A. Telfer, K.J. Williams, I.J. Stratford

Acknowledgments

The authors thank Mike Firth for the use of the metabolic network viewer, Radoslaw Polanski and Christopher Morrow for their helpful discussions and the Faculty of Life Sciences, the University of Manchester for making available the FACS and microscopy core facilities. The award of PhD studentships by BBSRC to A.L. Chadwick and K.G. Blount is gratefully acknowledged.

Grant Support

The work was funded by grants (to I.J. Stratford) from the MRC (G0500366) and AstraZeneca.

The costs of publication of this article were defrayed in part by the payment of page charges. This article must therefore be hereby marked *advertisement* in accordance with 18 U.S.C. Section 1734 solely to indicate this fact.

Received December 20, 2013; revised August 15, 2014; accepted September 19, 2014; published OnlineFirst October 3, 2014.

References

1. Gray LH, Conger AD, Ebert M, Hornsey S, Scott OCA. The concentration of oxygen dissolved in tissues at the time of irradiation as a factor in radiotherapy. Br J Radiol 1953;26:638–48.
2. Karar J, Maity A. Modulating the tumor microenvironment to increase radiation responsiveness. Cancer Biol Ther 2009;8:1994–2001.
3. Koch CJ, Kruuv J, Frey HE. Variation in radiation response of mammalian cells as a function of oxygen tension. Radiat Res 1973; 53:33–42.
4. Yasuda H. Solid tumor physiology and hypoxia-induced chemo/radioresistance: novel strategy for cancer therapy: nitric oxide donor as a therapeutic enhancer. Nitric Oxide 2008;19:205–16.
5. Pavlides S, Whitaker-Menezes D, Castello-Cros R, Flomenberg N, Witkiewicz AK, Frank PG, et al. The reverse Warburg effect: aerobic glycolysis in cancer associated fibroblasts and the tumor stroma. Cell Cycle 2009;8:3984–4001.
6. Hanahan D, Weinberg RA. Hallmarks of cancer: the next generation. Cell 2011;144:646–74.
7. Hirschhaeuser F, Sattler UG, Mueller-Klieser W. Lactate: a metabolic key player in cancer. Cancer Res 2011;71:6921–5.
8. Fulham MJ, Bizzi A, Dietz MJ, Shih HH, Raman R, Sobering GS, et al. Mapping of brain tumor metabolites with proton MR spectroscopic imaging: clinical relevance. Radiology 1992;185:675–86.
9. Hossmann KA, Mies G, Paschen W, Szabo L, Dolan E, Wechsler W. Regional metabolism of experimental brain tumors. Acta Neuropathol 1986;69:139–47.
10. Kennedy KM, Dewhirst MW. Tumor metabolism of lactate: the influence and therapeutic potential for MCT and CD147 regulation. Future Oncol 2010;6:127–48.
11. Paschen W, Djuricic B, Mies G, Schmidt-Kastner R, Linn F. Lactate and pH in the brain: association and dissociation in different pathophysiological states. J Neurochem 1987;48:154–9.
12. Yokota H, Guo J, Matoba M, Higashi K, Tonami H, Nagao Y. Lactate, choline, and creatine levels measured by vitro 1H-MRS as prognostic parameters in patients with non–small cell lung cancer. J Magn Reson Imaging 2007;25:992–9.
13. Halestrap AP, Price NT. The proton-linked monocarboxylate transporter (MCT) family: structure, function and regulation. Biochem J 1999;343:281–99.
14. Ovens MJ, Davies AJ, Wilson MC, Murray CM, Halestrap AP. AR-C155858 is a potent inhibitor of monocarboxylate transporters MCT1 and MCT2 that binds to an intracellular site involving transmembrane helices 7–10. Biochem J 2010;425:523–30.
15. Halestrap AP, Meredith D. The SLC16 gene family-from monocarboxylate transporters (MCTs) to aromatic amino acid transporters and beyond. Pflugers Arch 2004;447:619–28.
16. Juel C, Halestrap AP. Lactate transport in skeletal muscle—role and regulation of the monocarboxylate transporter. J Physiol 1999;517: 633–42.
17. Ullah MS, Davies AJ, Halestrap AP. The plasma membrane lactate transporter MCT4, but not MCT1, is up-regulated by hypoxia through a HIF-1alpha-dependent mechanism. J Biol Chem 2006; 281:9030–7.
18. Bonen A. The expression of lactate transporters (MCT1 and MCT4) in heart and muscle. Eur J Appl Physiol 2001;86:6–11.
19. Dubouchaud H, Butterfield GE, Wolfel EE, Bergman BC, Brooks GA. Endurance training, expression, and physiology of LDH, MCT1, and MCT4 in human skeletal muscle. Am J Physiol Endocrinol Metab 2000;278:E571–9.
20. Manning Fox JE, Meredith D, Halestrap AP. Characterisation of human monocarboxylate transporter 4 substantiates its role in lactic acid efflux from skeletal muscle. J Physiol 2000;529:285–93.
21. Bergersen LH. Is lactate food for neurons? Comparison of monocarboxylate transporter subtypes in brain and muscle. Neuroscience 2007;145:11–9.
22. Brooks GA. Lactate shuttles in nature. Biochem Soc Trans 2002; 30:258–64.
23. Pellerin L. Lactate as a pivotal element in neuron-glia metabolic cooperation. Neurochem Int 2003;43:331–8.
24. Sonveaux P, Végran F, Schroeder T, Wergin MC, Verrax J, Rabbani ZN, et al., Targeting lactate-fueled respiration selectively kills hypoxic tumor cells in mice. J Clin Invest 2008;118:3930–42.
25. Martinez-Outschoorn UE, Balliet RM, Lin Z, Whitaker-Menezes D, Howell A, Sotgia F, et al. Hereditary ovarian cancer and two-compartment tumor metabolism: epithelial loss of BRCA1 induces hydrogen peroxide production, driving oxidative stress and NFkappaB activation in the tumor stroma. Cell Cycle 2012;11:4152–66.
26. Fiaschi T, Chiarugi P. Oxidative stress, tumor microenvironment, and metabolic reprogramming: a diabolic liaison. Int J Cell Biol 2012;2012: 762825.
27. Pinheiro C, Albergaria A, Paredes J, Sousa B, Dufloth R, Vieira D, et al. Monocarboxylate transporter 1 is up-regulated in basal-like breast carcinoma. Histopathology 2010;56:860–7.
28. Chen H, Wang L, Beretov J, Hao J, Xiao W, Li Y. Co-expression of CD147/EMMPRIN with monocarboxylate transporters and multiple

Published OnlineFirst October 3, 2014; DOI: 10.1158/1535-7163.MCT-13-1091

drug resistance proteins is associated with epithelial ovarian cancer progression. Clin Exp Metastasis 2010;27:557–69.
29. Pinheiro C, Longatto-Filho A, Simões K, Jacob CE, Bresciani CJ, Zilberstein B, et al. The prognostic value of CD147/EMMPRIN is associated with monocarboxylate transporter 1 co-expression in gastric cancer. Eur J Cancer 2009;45:2418–24.
30. Pinheiro C, Longatto-Filho A, Scapulatempo C, Ferreira L, Martins S, Pellerin L, et al. Increased expression of monocarboxylate transporters 1, 2, and 4 in colorectal carcinomas. Virchows Arch 2008;452:139–46.
31. Kim HS, Masko EM, Poulton SL, Kennedy KM, Pizzo SV, Dewhirst MW, et al. Carbohydrate restriction and lactate transporter inhibition in a mouse xenograft model of human prostate cancer. BJU Int 2012; 110:1062–9.
32. Miranda-Gonçalves V, Honavar M, Pinheiro C, Martinho O, Pires MM, Pinheiro C, et al. Monocarboxylate transporters (MCTs) in gliomas: expression and exploitation as therapeutic targets. Neuro Oncol 2013;15:172–88.
33. Colen CB, Shen Y, Ghoddoussi F, Yu P, Francis TB, Koch BJ, et al. Metabolic targeting of lactate efflux by malignant glioma inhibits invasiveness and induces necrosis: an *in vivo* study. Neoplasia 2011;13:620–32.
34. Halestrap AP. e-letter: inhibiting lactate oxidation in tumor cells. J Clin Invest 2008;118 3930–42.
35. Busk M, Walenta S, Mueller-Klieser W, Steiniche T, Jakobsen S, Horsman MR, et al. Inhibition of tumor lactate oxidation: consequences for the tumor microenvironment. Radiother Oncol 2011;99:404–11.
36. Bueno V, Binet I, Steger U, Bundick R, Ferguson D, Murray C, et al. The specific monocarboxylate transporter (MCT1) inhibitor, AR-C117977, a novel immunosuppressant, prolongs allograft survival in the mouse. Transplantation 2007;84:1204–7.
37. Ekberg H, Qi Z, Pahlman C, Veress B, Bundick RV, Craggs RI, et al. The specific monocarboxylate transporter-1 (MCT-1) inhibitor, AR-C117977, induces donor-specific suppression, reducing acute and chronic allograft rejection in the rat. Transplantation 2007;84: 1191–9.
38. Le Floch R, Chiche J, Marchiq I, Naiken T, Ilic K, Murray CM, et al. CD147 subunit of lactate/H +symporters MCT1 and hypoxia-inducible MCT4 is critical for energetics and growth of glycolytic tumors. Proc Natl Acad Sci U S A 2011;108:16663–8.
39. Critchlow SE, Hopcroft L, Mooney L, Curtis N, Whalley N, Zhong H, et al. Pre-clinical targeting of the metabolic phenotype of lymphoma by AZD3965, a selective inhibitor of monocarboxylate transporter 1 (MCT1) [abstract]. In: Proceedings of the 103rd Annual Meeting of the American Association for Cancer Research; 2012 Mar 31–Apr 4; Chicago, IL: AACR; 2012. Abstract nr 3224.
40. http://science.cancerresearchuk.org/.
41. Swainston N, Golebiewski M, Messiha HL, Malys N, Kania R, Kengne S, et al. Enzyme kinetics informatics: from instrument to browser. FEBS J 2010;277:3769–79.
42. Williams KJ, Telfer BA, Shannon AM, Babur M, Stratford IJ, Wedge SR. Combining radiotherapy with AZD2171, a potent inhibitor of vascular endothelial growth factor signaling: pathophysiologic effects and therapeutic benefit. Mol Cancer Ther 2007;6:599–606.
43. Workman P, Aboagye EO, Balkwill F, Balmain A, Bruder G, Chaplin DJ, et al. Guidelines for the welfare and use of animals in cancer research. Br J Cancer 2010;102:1555–77.
44. Bensaad K, Tsuruta A, Selak MA, Vidal MN, Nakano K, Bartrons R, et al. TIGAR, a p53-inducible regulator of glycolysis and apoptosis. Cell 2006;126:107–20.
45. Gottlieb E, Vousden KH. p53 regulation of metabolic pathways. Cold Spring Harb Perspect Biol 2010;2:a001040.
46. Semenza GL. Regulation of metabolism by hypoxia-inducible factor 1. Cold Spring Harb Symp Quant Biol 2011;76:347–53.
47. Whitaker-Menezes D, Martinez-Outschoorn UE, Lin Z, Ertel A, Flomenberg N, Witkiewicz AK, et al. Evidence for a stromal-epithelial "lactate shuttle" in human tumors: MCT4 is a marker of oxidative stress in cancer-associated fibroblasts. Cell Cycle 2011; 10:1772–83.
48. Halestrap AP. The monocarboxylate transporter family—structure and functional characterization. IUBMB Life 2012;64:1–9.
49. Kennedy KM, Scarborough PM, Ribeiro A, Richardson R, Yuan H, Sonveaux P, et al. Catabolism of exogenous lactate reveals it as a legitimate metabolic substrate in breast cancer. PLoS ONE 2013;8: e75154.

Published OnlineFirst October 3, 2014; DOI: 10.1158/1535-7163.MCT-13-1091

Molecular Cancer Therapeutics

Inhibition of Monocarboxylate Transporter-1 (MCT1) by AZD3965 Enhances Radiosensitivity by Reducing Lactate Transport

Becky M. Bola, Amy L. Chadwick, Filippos Michopoulos, et al.

Mol Cancer Ther 2014;13:2805-2816. Published OnlineFirst October 3, 2014.